A Survey of Electron Probe Microanalysis Using Soft Radiations: Difficulties and Presentation of a New Computer Program for Wavelength Dispersive Spectrometry

M. Fialin
Université Pierre et Marie Curie

J. Hénoc
CAMECA, France

G. Remond
BRGM, France

Utah State University
MERRILL-CAZIER LIBRARY

A SURVEY OF ELECTRON PROBE MICROANALYSIS USING SOFT RADIATIONS: DIFFICULTIES AND PRESENTATION OF A NEW COMPUTER PROGRAM FOR WAVELENGTH DISPERSIVE SPECTROMETRY

M. Fialin[*], J. Hénoc[1], and G. Remond[2]

URA 736 CNRS, Université Pierre et Marie Curie, 75252 Paris Cedex 05, France
[1]CAMECA, 103 Boulevard Saint Denis, 92400 Courbevoie, France
[2]BRGM, Département DR/GGP, 45060 Orléans Cedex, France

Abstract

This paper aims to demonstrate that on-line peak integral technique with wavelength dispersive spectroscopy (WDS) provides accurate results with intensity measurement counting times as short as one or two minutes, owing to the high counting rates obtained with multilayer analyzers. A great advantage of a new computer program using this technique (available on SUN/UNIX work-stations operating Cameca SX-50 microprobes) consists in the original way that peak overlaps are treated. For each analytical point, overlapping counts emerging from an element B (B counts) are removed on-line from the measured raw counts in order to obtain the net counts corresponding to the element to be analyzed (element A). B counts are first measured on a proper standard containing B but not A.

The effects of chemical bonding on the shape and the shift of peaks is clearly seen in the analysis of fluorine in topaz and lithium fluoride. Self-absorption effects, which usually distort the high energy side of L-series soft radiations, are generally inconsistent with the direct measurements of peak area for k-ratio determination. A method based on the conventional area/peak factor concept is proposed for this purpose.

Key Words: Computer assisted treatment of soft radiations, on-line measurements of peak integrals, peak overlaps, K-series soft lines, L-series soft lines.

---

[*]Address for correspondence:
Michel Fialin
Centre d'Analyses par Microsonde CAMPARIS
Université P. et M. Curie - Tour 26 ét. 3,
4, Place Jussieu 75252 Paris Cedex 05 France
Phone No.: (33) 44 27 39 10
FAX No.: (33) 44 27 39 11

Introduction

Electron probe microanalysis (EPMA) of light elements ($Z < 10$) has been significantly improved during the past decade. The publication of sophisticated matrix effect correction models for data reduction, known as "phi-rho-z" models (e.g., PAP [12], PROZA [2]), together with new accurate tables of mass absorption coefficients (m.a.c.), has constituted the first meaningful step for this purpose.

The use of peak count ratios is based on the assumption that the ratio of peak to total band intensity is the same for both standard and unknown. In general, that is not the case for soft radiations. We propose a quantitative program for wavelength dispersive spectrometry (WDS) in which k-ratio determination using band area, instead of conventional peak measurements, can be obtained according to the user's choice. After a description of the main features of the method, some examples are given.

The power of the method in the treatment of overlapping line problems, common in light element analysis, is tested through analysis of carbon in uranium carbides and nitrogen in titanium nitrides.

Fluorine is still the most widely analyzed among the light elements in mineralogical and geological applications. Besides, this element is particularly interesting from a spectrometric point of view because of the changes which affect $K\alpha$ emission from an ionic (e.g., LiF) or a covalent (e.g., topaz) compound. This study will also discuss implications of the nature of chemical bonding in soft radiation EPMA.

The use of soft L-series bands is considered in the final section. Particular attention is drawn to self-absorption effects which strongly influence the behaviour of these emissions and consequently the count measurements.

Basic Features of the New Analytical Procedure

The need of a computer program including on-line measurements of band area for k-ratio determination

with WDS was initiated with the idea to offer to non-expert microprobe users an easy-to-operate tool for the completion of analytical sessions involving light elements [14]. It is now well known that the use of soft radiations for EPMA is hazardous unless both peak position and band shape changes between the specimen and the standard are taken into account. This implies the ability for quantitative programs to introduce a proper previously estimated area/peak factor (APF) each time a new compound is analyzed. Oxygen analysis to be performed on a wide variety of minerals is significant in this respect. Moreover, unexpected changes in composition within the same phase, with eventual large and rapid variations of the relevant APF, may lead to large analytical errors.

A great flexibility of the program consists in the opportunity to choose between peak and area measurement modes for each analyzed element. Elements being analyzed by mean of the peak height measurement procedure for obtaining the intensity of an X-ray line will be designated as "peak" elements. "Area" elements will refer to the elements for which the intensity of their characteristic X-ray lines is derived from the peak area measurement obtained by on-line summation of the counts contained in each successive channel analyzed by stepping monochromator. "Peak" elements can be independently measured while spectra acquisitions for the others are completed. Owing first to the short counting time used in area modes and second to the less numerous "area" elements which usually compose an analytical sequence (for mineralogical and geological applications at least), no dramatic increase in analytical time as compared to conventional WDS procedure was noted, assuming a proper management of available spectrometer time is made.

Spectra are digitally recorded and counts per channel are corrected for dead-time before the total channel counts are accumulated. The background contribution is removed from the raw counts using a linear or a parabolic interpolation based on the least-square method applied to a proper set of counts pertaining to both outer regions of the spectral range scanned.

The treatment of peak overlap constitutes an important and innovative part of this program. The method proposed consists of an estimation of the band contribution emitted from an element B, which overlaps the analyzed band, emitted from an element A. The overlapping band must be diffracted in the first order by the monochromator {multiple orders are eliminated by proper setting of the single channel pulse height analyzer (PHA)}.

The intensity I_s of the overlapping line emitted from B is measured on a standard free of A (named overlap standard in this text) with the same acquisition parameters as for A. The relative intensity k of the element A, corrected for overlapping, is given by:

$$k = \{I_A - I_s (C_u / C_s) (PAP_u / PAP_s)\} / I_{std}, \quad (1)$$

where:

I_A, I_s, I_{std}: intensity of the line measured on the unknown (with overlapping included), the overlap standard and the analytical standard (C/s/nA), respectively;

C_u, C_s: weight fraction of the element B in the unknown and the overlap standard, respectively; and

PAP_u, PAP_s: correction parameters of the line for the unknown and the overlap standard, respectively.

In practice, I_s is measured and PAP_s is calculated using a program written for this purpose. Both quantities are stored into a file for further use in the quantitative program. During the analysis of the specimen, PAP_u depends on the chemical composition of the specimen. A first execution of the Pouchou and Pichoir's procedure (PAP) [12], using I_A/I_{std} (for the input relative intensity of element A), gives an estimate of the chemical composition. PAP is then run again in order to calculate PAP_u and k. The expected composition of the specimen is obtained after a third run of PAP.

Emergent B counts (from both the specimen and overlap standard) are treated by PAP using the same spectral parameters as A counts (line energy, mean excitation energy, critical ionization energy, etc.): PAP considers the overlapping line as the analyzed one, assuming the latter is emitted from B atoms.

Thus, a precise physical description of the overlapping line, which may not be easily available, is not necessary for this overlap correction method. Moreover, it must be noted that the knowledge of band shapes is not important here, since the method is based on the comparison of measured area counts. Only anomalies of emission for relevant lines (e.g., changes in electronic transition probabilities) between each one of the specimens involved could lead to failure of the proposed procedure.

Examples and Discussion

Treatment of peak overlaps

The first example deals with peak overlap induced perturbations in light element analysis. Figure 1 shows the digitally recorded spectra emitted from diamond and pure uranium targets within the range 180-590 eV. While the C $K\alpha$ band can be immediately recognized from the diamond spectrum, such is not the case for the U line, which is generally not mentioned in the tables available to analysts. In searching the literature, it appears that electronic transitions from O_{IV} to N_{VI} levels may be involved in this emission [3]. Since no official

154

1 Ni/C
15 kV

········ diamond
—— U metal (x8)

sin Θ

.221   .733

.46 .471

2 UC$_2$/C (diamond)

carbon
concentration
20 (wt %)

15

10

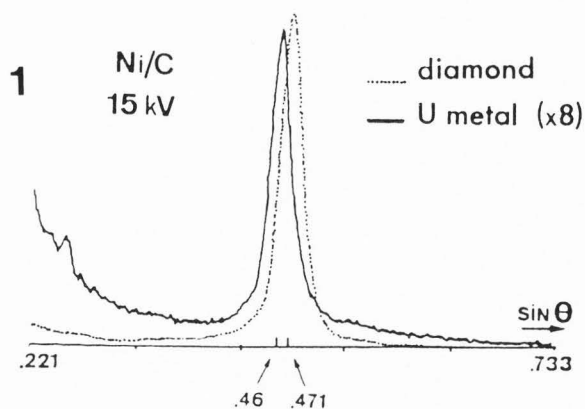UC$_2$ (9.2 wt% C)

5   10   15   20   kV

Figure 1 (above). Comparison of spectra emitted from diamond and pure uranium targets within the full wavelength range of one of the microprobe spectrometers equipped with a Ni/C multilayer (2d spacing = 9.5 nm). The strong overlap between C Kα and U Nx (see text) bands is clearly shown. The peak shift measured is 6.6 eV. Note the characteristic asymmetry of the U Nx band.
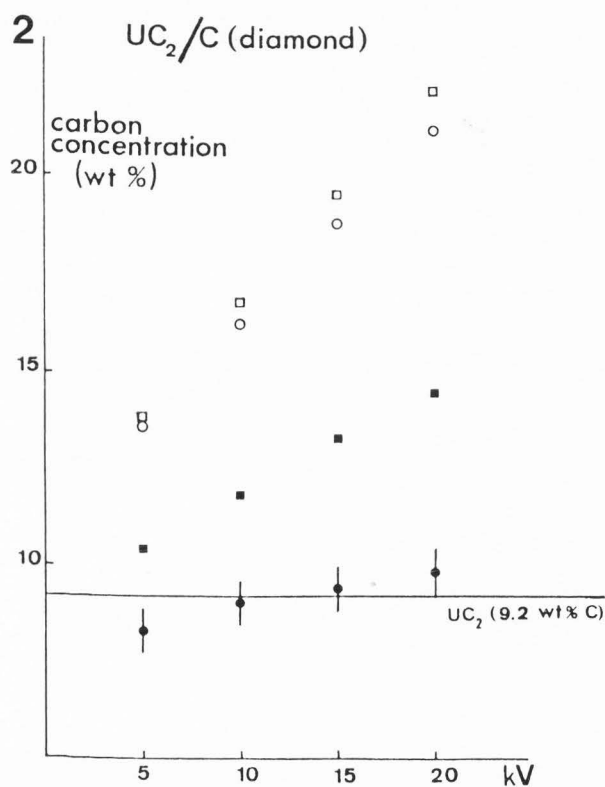
Figure 2 (below). Results of carbon analysis in UC$_2$ with diamond as the standard at 5, 10, 15, and 20 kV. **Circles**: area measurements; **squares**: peak measurements; **solid symbols**: with overlap correction (pure U as the overlap standard); and **open symbols**: without overlap correction. Bars (for area with overlap points) correspond to 2σ precision. Only average values are shown for others. **Operating conditions**: 20 nA at each voltage. PHA in the integral mode. Band acquisition: 0.1 second per channel, 1000 channels (100 seconds effective counting time per spectrum). Spectral range of interest (ROI) scanned: 20000 steps (10000 steps on each sides of the peak; 1 step corresponds to a variation of sinθ = 10^{-5}). Counting rates for UC$_2$: of the order of 10^5 counts per band area (contribution of the off-peak bremsstrahlung removed), compared to 10^4 c/s on peak. Area data provide the same statistics as peak data obtained after 10 seconds counting time.

----

measurements with overlap correction is used (solid circles). Accurate results are obtained in the voltage range 10-15 kV, as often noted in light element analysis. Also, the problem of the mass absorption coefficient (m.a.c.) determination for C Kα in U has to be considered. Owing to the multitude of electronic levels present in an heavy atom (such as U) together with the uncertainties regarding the knowledge of their physical properties (ionization energies, electronic populations, etc.), the tabulated m.a.c. are often doubtful, when the emitter band energy (C Kα: 0.284 KeV) is below the M$_V$ edge of the absorber (U M$_V$: 3.55 KeV) [8]. The set of m.a.c. used in this work is based on polynomial fits to Henke *et al.*'s tables [9] available in our PAP model. The m.a.c. value used for C Kα in U is 6440 cm^2/g. A difference between both the tabulated and the "true" values could explain the obvious dependence of the measured concentration on the primary beam energy.

An interesting application of the new program is illustrated in Figure 3. Small inclusions (maximum dimension: 10 mm) found within a pure U plate were to be characterized. A preliminary qualitative analysis had shown that they were uranium carbide. The operating conditions chosen were the same as previously used for UC$_2$ (Figure 2); the beam voltage chosen was 10 kV. The carbon profiles (wt% and at%) plotted in Figures 3a

label can be attributed to this line, we refer to it as U Nx. As Figure 1 shows, the contribution of U Nx to C Kα bands will strongly influence carbon analysis of U-rich compounds such as uranium carbides, e.g., UC$_2$ (90 wt% U) or UC (95.2 wt% U).

The results of carbon analysis in UC$_2$ using pure U as the overlap standard are plotted in Figure 2. Note the strong and increasing deviations with voltage, affecting apparent carbon concentrations, when measurements are performed without overlap correction (hollow symbols), or when the conventional peak method (solid squares) is used even if the overlap correction is applied. This increase is much less when the method based on area
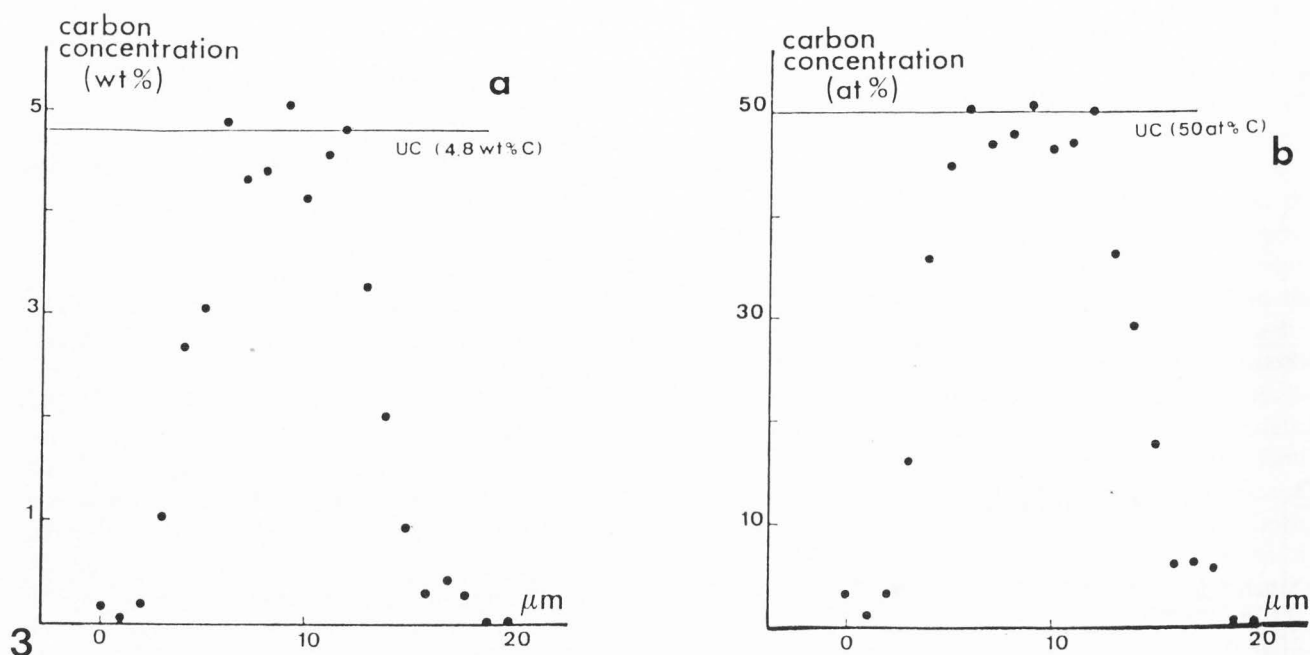
Figure 3. Results for carbon analysis (wt% in **a** and at% in **b**) on a uranium carbide precipitate within uranium matrix at 10 kV using the same operating conditions as in Figure 2. Analysis was performed across the precipitate at 1 μm steps. Uranium was analyzed with the peak mode (Mα band, PET monochromator) while C Kα band was completed.

Table 1. Results of nitrogen analysis in TiNOx (wt% contents: N: 13.9; Ti: 78.6; and O: 7.5) without (**1**) and with (**2**) matrix effect correction for the overlapping band using CrN$_x$ as standard and Ti and TiC as overlap standards. n.d.: not determined. Numbers in parenthesis indicate the relative % error compared to the expected value. Operating conditions: 10 kV, 50 nA, PHA integral. N Kα band acquisition: 1000 channels, 0.07 sec./chan. ROI = 8000 steps.

		Concentration (wt%)				
	Overlap	No overlap correction		Overlap correction		
Standard	Standard	peak	area	peak	area (1)	area (2)
CrN$_x$ (13 wt% N)	Ti	20.00 (44)	21.20 (53)	16.15 (16)	14.35 (3.2)	14.55 $\pm$ 0.41 (4.7)
	TiC			n.d.	18.20 (31)	14.75 $\pm$ 0.43 (6)

and 3b represent an analytical profile across one of the inclusions. These results clearly point to UC as the chemical formula for these carbides. The carbon concentration falls correctly to zero on each side of the inclusion, which demonstrates the efficiency of the overlap correction. Indeed, an equivalent "carbon" concentration as large as 8 wt% is found for pure U, if this correction is not applied. This method could be used to show eventual carbon gradients around inclusions.

The above analytical sequence was automatically performed, and is easy compared with the usual WDS method based on peak measurements. In the latter method, almost every analytical point would necessitate a different APF to be applied to the peak k-ratios

together with a displacement of the spectrometer in order to account for the band shape changes and the shift in position of the line of interest from U to UC, respectively.

The choice of the overlap standard is of great interest to evaluate as precisely as possible the stray counts to be removed from the characteristic band of an unknown. As an example, the results of nitrogen analysis within a Ti-rich compound, for different analytical conditions, are summarized in Table 1. The strong Ti Lι overlap on N Kα is well-known to microprobe users. Errors as large as 50% on N wt% concentrations are noted here if no overlap correction is applied. Pure Ti, used as the overlap standard, leads to satisfactory results (less than 5% error) which, however, could be even

better, in our opinion, if the surface oxygen contamination of the metal standard could be completely removed. Indeed, the presence of such oxidized surfaces cannot be avoided for Ti alloys [6] and reduces the emitted Ti $K\alpha$ count rates which, in this example, leads to underestimation of overlapping counts and thus to overestimated N concentrations.

Table 1 clearly illustrates the dangers of using TiC as an overlap standard. In TiC, Ti $L\iota$ is strongly absorbed by C atoms (such as N $K\alpha$ should be within an hypothetical NC compound ; m.a.c. of N $K\alpha$ in C: 25500 cm^2/g). In this respect, note the strong changes in the results according to whether raw or matrix effect corrected Ti $L\iota$ counts are used. This example shows the importance of the PAP_u/PAP_s factor in eq. (1). For pure Ti, no such problem arises due to the more or less similar corrections for Ti $L\iota$ emitted from both specimens.

An example of fluorine analysis

Owing to the usual mechanical limits of available WDS spectrometers, fluorine is the only light element whose $K\alpha$ band can be recorded using a thallium acid phthalate (TAP) monochromator (2d spacing = 2.5745 nm). The improved resolution of TAP as compared to, for instance, that of the Ni/C multilayer used above provides an opportunity to detail with more precision the shape of the band of interest. Figure 4a presents a comparison of the F $K\alpha$ bands emitted from a strongly ionic compound, LiF, and a topaz, in which the ionic nature of the chemical bond F-Al (the only bonding in which F atoms are involved) is less pronounced. As expected for a low energy band emitted from an almost ionic compound, the peak is shifted towards low energy (0.4 eV) for LiF compared to topaz. A strong band shape alteration {APF (topaz/LiF) = 1.47} is also noted. On the high energy side of the peak, two emissions attributed to shake-off processes are clearly shown for LiF. $K\alpha_{3,4}$ (3,4 eV from the peak) corresponds to the radiative de-excitation of F^- ions in the presence of two vacancies in the L level ($KL_{2,3} \rightarrow L^2_{2,3}$ transitions) [7], whereas $K\alpha_{5,6}$ (8.8 eV from the peak) is due to a third L-vacancy ($KL^2_{2,3} \rightarrow L^3_{2,3}$ transitions). Note the strong weight of these satellites with respect to the main band. A first indication of the "less ionic nature" of F $K\alpha$ band emitted from topaz is the reduction of the satellite emission which can be deduced from the obvious loss in intensity of $K\alpha_{5,6}$ band (the $K\alpha_{3,4}$ doublet is not resolved here and appears as a shoulder of $K\alpha_{1,2}$). Indeed, as underlined by Aberg [1], the stronger the atomic character of valence states (ionic bonds), the higher the probability of multiple ionizations of these states.

Furthermore, a strong shoulder appears at about -3 eV of the main peak for topaz, indicating the presence of an unresolved band. The contribution of filled p-character states due to the mixing of F 2p and Al 3sp valence states (to form the covalent F-Al bond) is certainly responsible for this low energy satellite. This interpretation can be justified by an investigation of the Al $K\beta$ band which originates from the same set of valence orbitals as F $K\alpha$. A comparison of Al $K\beta$ lines emitted from pure Al and topaz is presented in Figure 4b. Shake-off doublet satellites, $K\beta_{3,4}$ and $K\beta_{5,6}$, are particularly well resolved for pure Al. The main band $K\beta_{1,3}$ is shifted -5 eV for topaz with respect to the metal, which shows that Al 3p states are almost completely hybridized (mixed) with F 2p and O 2p states (Al atoms are surrounded by four O and two F atoms in topaz). Both sets of F 2p - Al 3p and O 2p - Al 3p p-like states give rise to two distinct emissions (unresolved here) to form the $K\beta_{1,3}$ band. Moreover, two satellites at -15 eV and -20 eV from the main peak are clearly shown for topaz. They originate from p-like states due to the mixing of Al 3p with O 2s and F 2s states, respectively. The energy differences found between Al $K\beta$ and these satellites agree fairly well with those measured in Al_2O_3 (-16 eV) [5] and AlF_6 (-21 eV) [15].

The strong ionic nature of LiF is consistent with most fluorine atoms as F^- ions. Furthermore, neutral F atoms are present in topaz in which the transfer of charge (the stronger this transfer, the more ionic the bonding) is not as complete. These differences in F 2p electronic population have an influence upon the transition probabilities occurring from these levels. As a consequence, fluorine analysis in topaz using LiF as the standard should lead to underestimated experimental k-ratios with respect to the calculated ones. Figure 5 shows that it is not the case. This feature can be understood in looking at the height of the low energy satellite (about 50% of the main peak) which demonstrates the almost but not complete charge transfer upon F sites in topaz. Thus, the weak differences in F 2p populations between specimens cannot be explained by anomalies in $K\alpha$ intensity ratios, whereas strong changes in band shape are noted.

F $K\alpha$ k-ratios for topaz/LiF are plotted in Figure 5 using a conventional TAP crystal and a W/Si multilayer (2d spacing = 6 nm). Owing to the very different conditions for fluorine analysis offered by each one of these monochromators (high reflectivity, low resolution power for W/Si, the opposite characteristics for TAP), a comparison of the corresponding results is a good test for the reliability of the method. Both good accuracy and statistics, using on-line area measurements, were obtained with 40 and 130 seconds as the effective counting time per spectrum acquisition for W/Si and TAP, respectively (see Figure 5 caption for details).
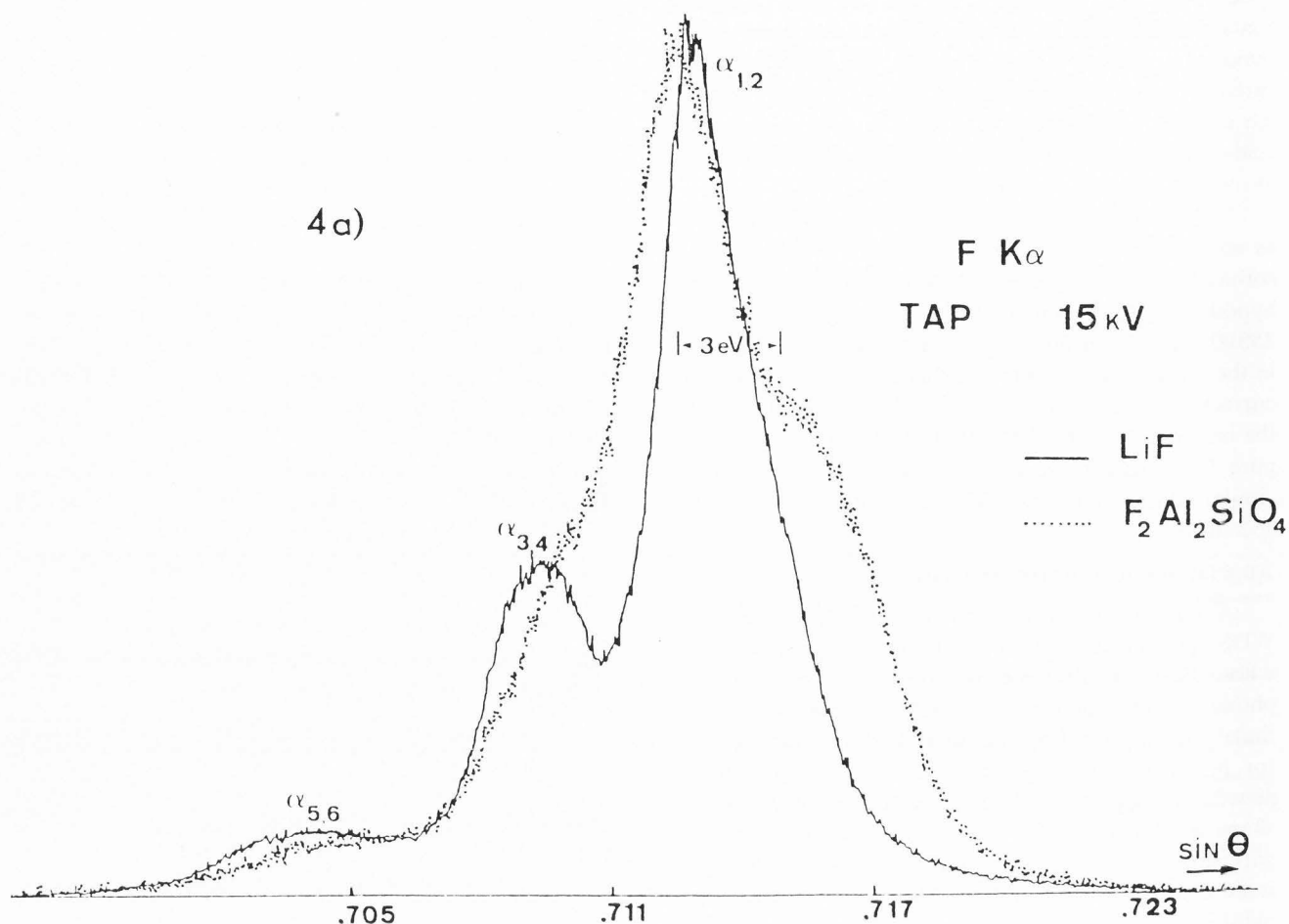
M. Fialin, J. Hénoc, and G. Remond

Figure 4. a (above). Comparison of F Kα bands emitted from LiF and topaz. Operating conditions: 1000 channels, 1 sec./chan., beam current: 160 nA. Both the unresolved low energy satellite, at 3 eV from the peak, and the peak shift towards high energies with respect to the ionic compound LiF, are noted. b (right). Comparison of Al Kβ bands emitted from pure Al and topaz, recorded in the second order reflection of a TAP monochromator. Operating conditions: 1000 channels, 7 sec./chan., 200 nA. Note the shift towards low energies (5 eV) of the main band for topaz with respect to pure Al, together with the presence of two satellites at -15 eV and -20 eV.
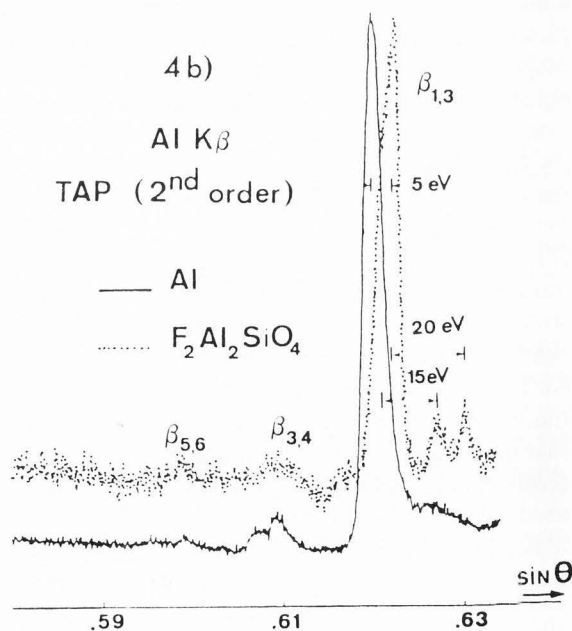
Some problems with the use of L-series soft lines

L-series lines of Cu and Zn are often useful for sulfide analysis in which many elements have to be analyzed and optimally distributed over the available spectrometers. These soft radiations (< 1 keV) are affected, as are the Kα radiations of light elements, by both
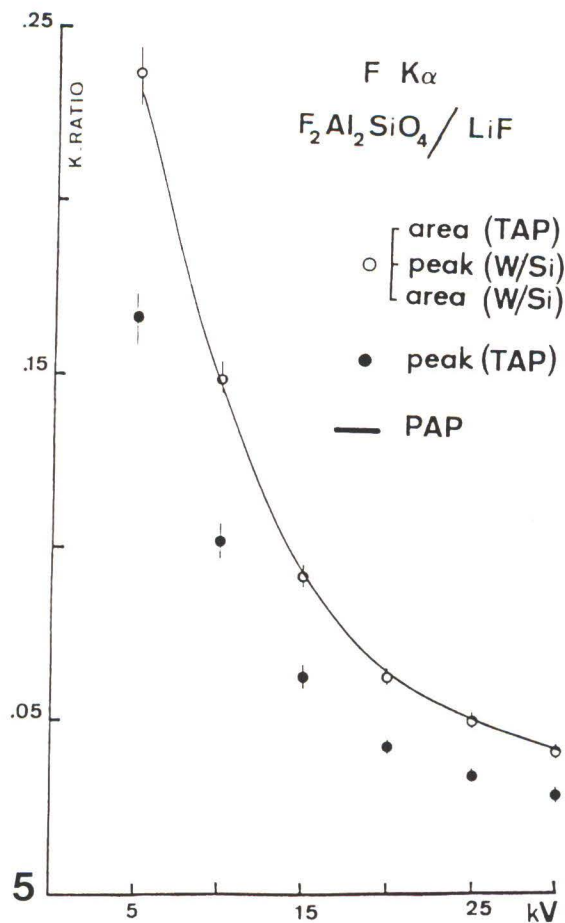
Figure 5 (above). Plot of Kα k-ratios for topaz (20.65 wt% F) with LiF as the standard in the voltage range 5-30 kV. Operating conditions: 10 nA at each voltages; PHA integral for TAP, differential for W/Si (1 V window centered on the PHA peak). **Band acquisition, TAP:** 0.13 sec./chan., 1000 channels, Region of interest (ROI) = 5000 steps; peak count rate = 100 c/s, total area counts = 1500. **Band acquisition, W/Si:** 0.04 sec./chan., 1000 channels, ROI = 5000 steps; peak count rate = 1000 c/s, total area counts = 7000. The setting of severe PHA conditions for W/Si is necessary in order to eliminate the contribution of the Al Kα second order reflection which occurs at 3000 steps from F Kα. Note, for TAP, the differences in k-ratios between peak and area measurements (APF = 1.47). Owing to its poor resolution compared to TAP, no difference is noted for W/Si between both acquisition modes.

Figure 6 (right). Plot of Cu Lα k-ratios for chalcopyrite/cuprite. The m.a.c. used are tabulated except that of Cu Lα in Fe which was taken as 12800 cm²/g (13230 tabulated).

spectroscopic (band property changes) and matrix effect problems. Unfortunately, other serious difficulties arise with these lines, which render quantitative analysis hazardous [14]. This last point is illustrated in Figure 6 which presents plots of Cu Lα k-ratios measured from a chalcopyrite (CuFeS$_2$) using a cuprite (Cu$_2$O) as the standard. Both specimens are semiconductors (band-gap width ∼ 2 eV) and neither lack of electrical conductivity nor charge buildup under irradiation were noted. The main feature is the surprisingly good results obtained using the peak as opposed to the area modes. In the peak mode, a constant 3% error from the theory is noted (35.2 wt% Cu instead of the expected 34.2 wt%) over the voltage range 5-30 kV, whereas the area mode data are characterized by an increasing error, from 8% at 5 kV to 20% at 30 kV. The observations of the relevant Cu Lα spectra compared in Figure 7 show why the use of raw area k-ratios is erroneous.

Voltage-dependent distortions affect the high energy side of the Cu Lα band in the region of the Cu L$_{III}$ edge, with stronger influence for cuprite. These effects are due to strong changes in Cu Lα self m.a.c. on each side of the Cu L$_{III}$ edge, which induce a differential absorption between the photons emitted above (highly

159

7 a)   Cu Lα   TAP   CuFeS₂

7 b)   Cu Lα   TAP   Cu₂O
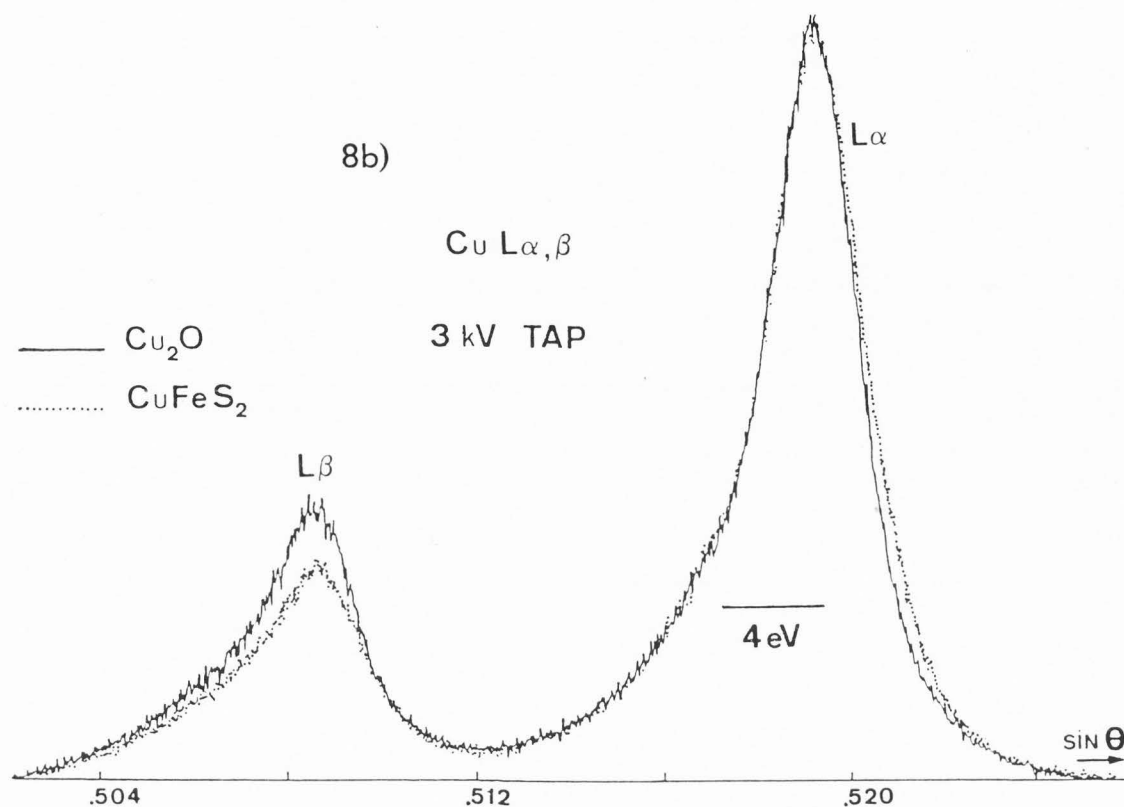
8a)   Cu Lα,β   15 kV   TAP

— Cu₂O
.... CuFeS₂
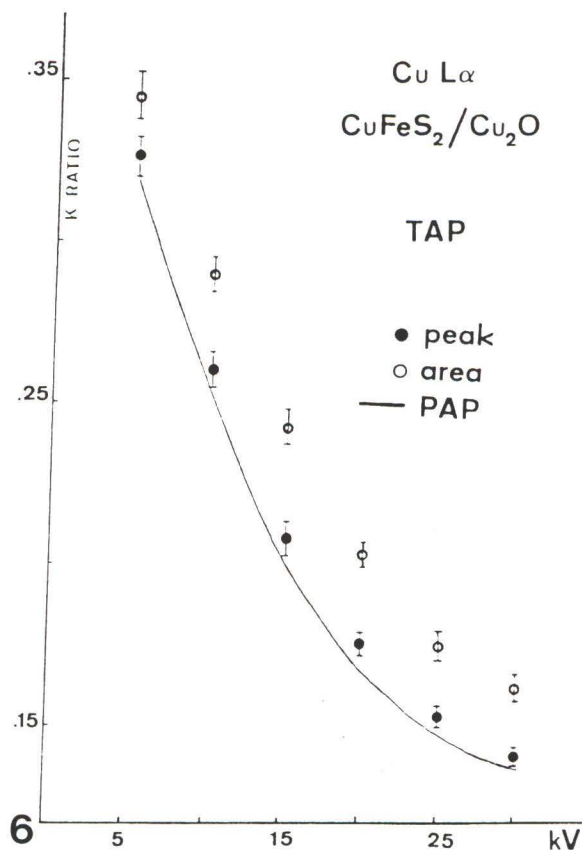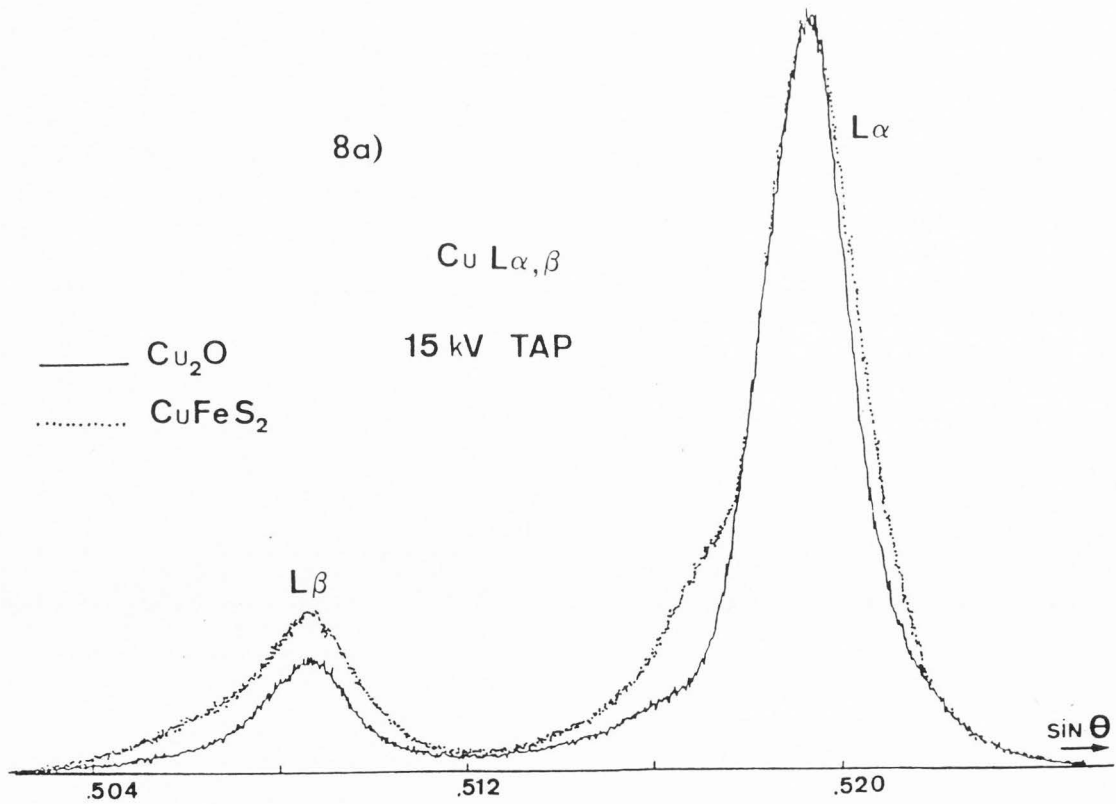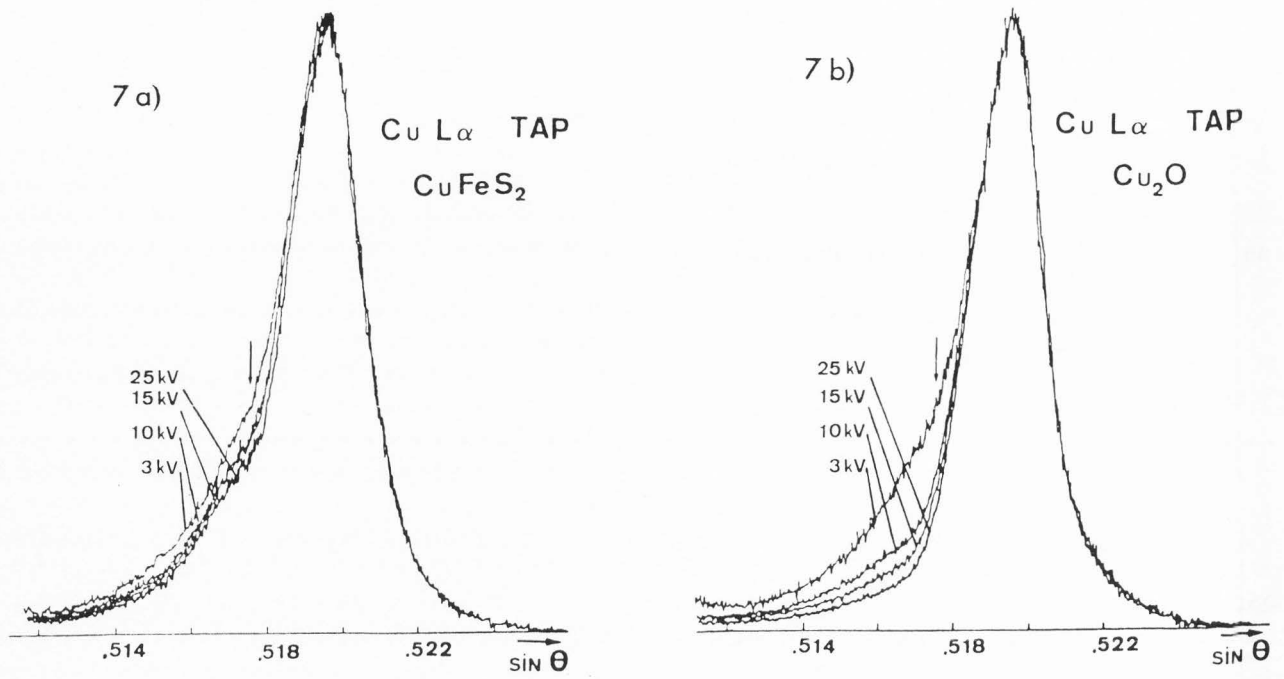
Figure 7 (facing page, above). Effects of the self-absorption on the shapes of Lα bands emitted from chalcopyrite (a) and cuprite (b). Arrows indicate the approximate position of the Cu L_{III} edge. In order to prevent eventual changes in band shapes due to dead-time induced losses of detection at high counting rate, the beam current was adjusted so as to obtain a constant peak counting rate of 1500 c/s for each one of the recorded spectra (600 channels, 2 sec./ chan.).

Figure 8 (a: facing page, below; b: this page, above). Comparison of Cu Lα and Lβ bands emitted from chalcopyrite and cuprite at 15 kV (a) and 3 kV (b). Voltage dependent distortions of the Lα high energy side is characteristic of self-absorption, whereas changes in Lβ/Lα intensity ratio may also be due to CK transitions (transfer of ionization from L_{II} to L_{III} levels) or electron transfer between M_{IV} and M_V levels.

---

absorbed) and below (weakly absorbed) this edge, respectively. The higher the self-absorption conditions (both high voltage and Cu contents), the stronger the distortions. Indeed, changes represent 22 % of the total band area at 25 kV (with respect to 3 kV for cuprite) as compared with 8 % for chalcopyrite. For further details concerning self-absorption effects on L-series soft emission spectra, the insightful paper by Liefield [11] is recommended.

Lα and Lβ lines are situated on both sides of the L_{III} edge. Figure 8a shows the changes in the Lβ/Lα intensity ratio between the two specimens at 15 kV: the stronger the self-absorption, the lower this ratio. At 3 kV (Figure 8b), self-absorption is low and no obvious

difference on the band high energy side is noted. Surprisingly, Lβ/Lα is now lower for chalcopyrite. Indeed, it would be expected at least that this ratio remains slightly higher than that of cuprite. In a first step, the contribution of Coster-Kronig (CK) transitions which lead to a transfer of ionization from L_{II} to L_{III} levels (with ejection of a 3d electron), could be involved in such an increase of Lα with respect to Lβ intensities. CK transitions induce the buildup of satellites in the high energy side of the band, which correspond to the increase in energy of the emission line in the presence of the 3d vacancy. According to Bonnelle [4], the total satellite band (both CK and shake-off) ranges approximately from 1 to 4 eV from the peak for pure

Cu. The increase in CK events for chalcopyrite might be accompanied by a more or less obvious increase of the satellite band intensity, which cannot be demonstrated by our spectra.

A second interpretation deals with changes in balance of the electronic population of M_{IV} and M_V levels (the initial levels involved in $L\alpha$ and $L\beta$ bands). Indeed $L\alpha_1$ intensity is favored by a transfer of electron from M_{IV} to M_V with respect to $L\alpha_2$ and $L\beta$. Besides, changes in valence band properties due to this electronic reorganization could be, in part, responsible for the voltage independent band shape difference noted in the low energy side of the main band between both specimens.

The actual problem with electron probe microanalysis using soft L-series lines pertains to the accurate measurements of the band area. For that purpose, raw area data used will be first freed of self-absorption effects and then will take into account eventual changes in $L\beta/L\alpha$ due to the above mentioned phenomena. The last point can be easily satisfied if the total $L\alpha + L\beta$ area is used. According to Liefield [11], distorting self-absorption effects may be eliminated using an absorption minimizing instrumental geometry (normal-incidence electron beam and normal take-off angle for photons with beam electrons of near-line threshold energy, i.e., 930 eV for Cu L_{III}). Additionally, since commercial microprobes do not offer the above geometry (take-off angle = 40 degrees), measurements are obviously inconsistent with the use of such very low voltages. The limitations are well known: beam instabilities, low nominal counting rates, and preponderant stray contribution of the imperfect and contaminated surface with respect to bulk emissions; the usual method based on APF measurements appears to be the only way to proceed. We propose a method in which the APF of interest is deduced after an extrapolation of experimental data to "zero self-absorption effects" is made.

For that purpose, we introduce a parameter named R (whose expression is given in Table 2) which accounts for changes in $L\beta/L\alpha$ ratios between the unknown and the standard. The aim of the method is to associate to the measured APF at a given voltage a theoretical value, R_{self}, which estimates R if self-absorption is the only cause of these changes ($R_{self} = 1$ when self-absorption is eliminated). Difficulties in the determination of R_{self} arise due to the doubtful value of the Cu $L\beta$ self m.a.c. This coefficient is often not tabulated and available values can strongly differ: for instance, 6500 cm^2/g can be found from Leroux and Thinh tables [10] as compared to 9600 cm^2/g in Heinrich [8].

In this study, we have adjusted this m.a.c. in order to obtain no difference between R_{self} and the measured value R_{exp} over a wide voltage range (Table 2). Indeed, no voltage dependence of R is expected (for the usual

Figure 9 (facing page, left). **a**. Plot of measured APF for Cu $L\alpha$ emitted from chalcopyrite and cuprite at 3, 10, 15, and 25 kV (numbers in parenthesis) versus R_{self}. Extrapolated APF for "zero self-absorption effects" ($R_{self} = 1$) are shown when either $L\alpha$ or $L\alpha + L\beta$ are considered. **b**. Plot of Cu $L\alpha$ k-ratios obtained after the above extrapolated APF were applied to peak k-ratios from Figure 6. Full circles: APF = 0.97 ($L\alpha + L\beta$); open circles: APF = 1.04 ($L\alpha$); solid line: PAP

Figure 10 (facing page, right). Same as Figure 9; pure Cu is used instead of cuprite.

----

voltage range used in EPMA at least) if self-absorption is removed. A value of 8000 cm^2/g has been found satisfactory in this respect.
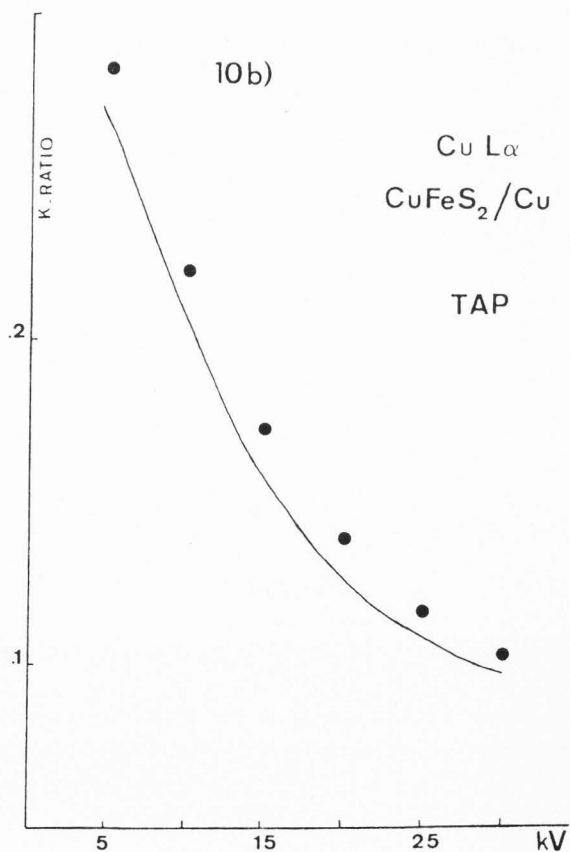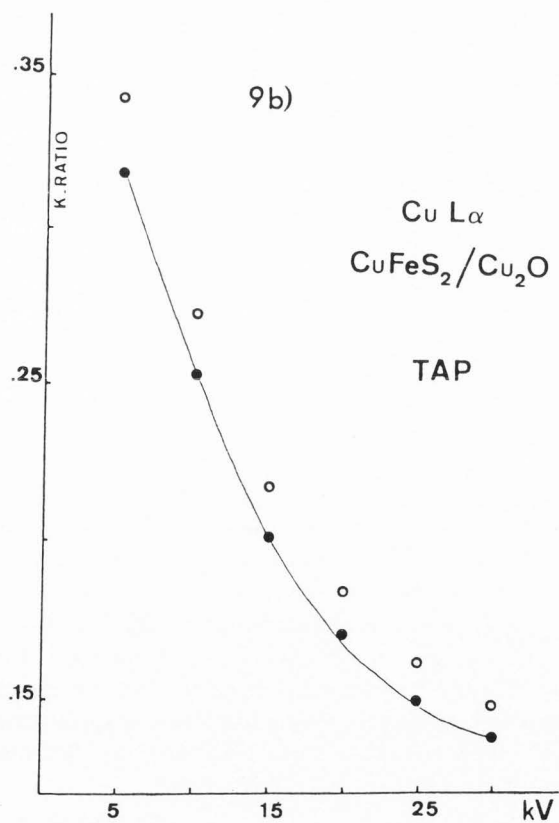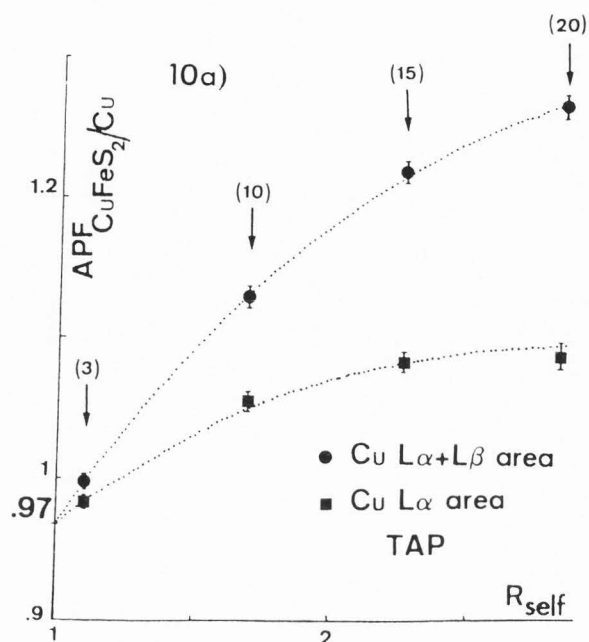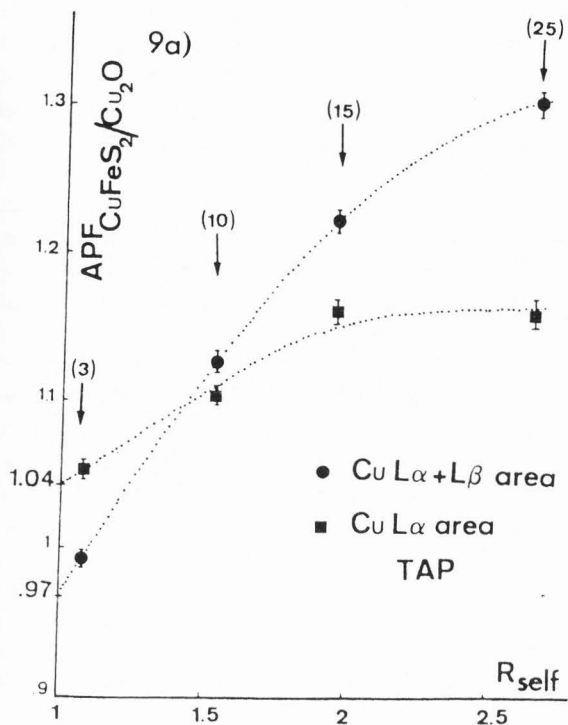
Figure 9 shows the relevant results of the method. Extrapolated APF to $R_{self} = 1$ (0.97) can be found on Figure 9a after measurements at 3, 10, 15, and 25 kV. Note the very different values are obtained depending on whether $L\alpha$ or $L\alpha + L\beta$ bands are used. Cu $L\alpha$ k-ratios for $CuFeS_2/Cu_2O$ are plotted in Figure 9b over the voltage range 5-30 kV. The comparison experimental-theoretical is quite satisfactory in this case.

Figure 10 shows the same results as Figure 9 except that pure Cu is now used as the standard. The important point in Figure 10a is that differences are no longer found in extrapolated APF values between both $L\alpha$ and $L\alpha + L\beta$ measurements (self-absorption only responsible for $L\beta/L\alpha$ changes). Contrary to Figure 9b, k-ratios plotted in Figure 10b present a constant experimental-theoretical shift of 8%. This situation could be compared with that described by Pouchou and Pichoir [13] for the case of the soft Ni $L\alpha$ band for analysis of Ni-Zn and Ni-Al alloys. Overestimation of the order of 10% for experimental results compared with theory were noted. It was assumed by these authors [13] that the 3d-2p transition probability was increased for Ni atoms

Table 2. Changes in Cu $L\beta/L\alpha$ ratios between chalcopyrite and cuprite at different voltages. R = $\{(IL\beta/IL\alpha)_{unk.} / (IL\beta/IL\alpha)_{std}\}$. R_{exp} : measured value of R. R_{self} : theoretical parameter giving the effect of the self-absorption on the $L\beta/L\alpha$ ratio changes.

kV	R_{exp}	R_{self}	Δ (%)
3	0.8	1.08	29.8
10	1.13	1.53	30.0
15	1.44	1.95	30.0
25	1.96	2.66	30.3

9a)

APF_{CuFeS_2}/Cu_2O

(3) (10) (15) (25)

R_{self}

● Cu Lα+Lβ area

■ Cu Lα area

TAP

10a)

APF_{CuFeS_2}/Cu

(3) (10) (15) (20)

R_{self}

● Cu Lα+Lβ area

■ Cu Lα area

TAP

9b)

K.RATIO

Cu Lα

$CuFeS_2/Cu_2O$

TAP

kV

10b)

K.RATIO

Cu Lα

$CuFeS_2/Cu$

TAP

kV

within alloys with respect to pure metal. As long as no further progress in solving this difficult problem is found, a similar hypothesis may be proposed for the above example.

Conclusion

K-ratio determination based on band measurements was, up to now, the characteristic feature of energy dispersive systems. A transposition of this method to WDS for the computer assisted treatment of soft radiations with the powerful available instruments can be reasonably considered if the conventional peak mode, for more energetic lines, is also available in quantitative programs. Indeed, this "hybrid" technique induces no dramatically long durations for measurements assuming the optimization of the analytical procedure, in particular when multi-element analyses have to be performed.

The program package proposed can efficiently treat most problems arising from light element EPMA. On the other hand, the use of soft L-series lines is hazardous because of self-absorption-induced biases. These effects could be minimized if standard and specimen are chosen with comparable contents of the analyzed element. If this action is not possible, preliminary calculations should be made in order to correct measured k-ratios for self-absorption. The method described above for this purpose is based on precise measurements of $L\alpha$ and $L\beta$ intensities. This necessitates that both emissions are sufficiently separated, a condition which renders the use of multilayers as monochromators inoperative.

Acknowledgements

References

[1] Aberg T (1967) Theory of X-ray satellites. Phys. Rev. **156**-1, 35-41.

[2] Bastin GF, Heijligers HJ (1991) Quantitative electron probe microanalysis of ultra-light elements (boron-oxygen). In: Electron Probe Quantitation. Heinrich KFJ, Newbury DE (eds.). Plenum Press, New York, 145-161.

[3] Bearden JA, Burr AF (1967) X-ray wavelengths. Review of Modern Physics **39**-1, 78.

[4] Bonnelle C (1966) Contribution à l'étude des métaux de transition du premier groupe, du cuivre et de leurs oxydes par spectrométrie X dans le domaine de 13 à 22 Å (Contribution to the study of the first series metals, copper and oxides by means of X-ray spectrometry in the 13 to 22 Å). Doctorate Thesis, University of Paris. Masson and Co., Paris, France.

[5] Cauchois Y (1968) Sur les spectres X des métaux - quelques commentaires et exemples (On metals x spectra - Some comments and examples). In: Soft X-ray Band Spectra. Fabian DJ (ed.). Academic Press, London, UK, 71-79.

[6] Goldstein JJ, Choi SK, Van Loo JJ, Heijligers HJM, Dijkstra JM, Bastin GF (1991) The influence of surface oxygen contamination of bulk EPMA of oxygen in ternary titanium-oxygen compounds. In: Microbeam Analysis, 1991. San Francisco Press, 57-58.

[7] Hayasi Y (1976) On the satellites of the $K\alpha$-doublet of fluorine in lithium fluorides. Int. Conf. Phys. X-ray Spectra. NBS publication, Gaithersburg, MD, 351.

[8] Heinrich KFJ (1989) Paramètres en microanalyse par sonde électronique (Parameters in electron probe microanalysis). In: Microanalyse par sonde électronique: aspects quantitatifs. Publ. ANRT, Paris, B1-B24.

[9] Henke BL, Lee P, Tanaka TJ, Shimabukuro RL, Fujikawa BK (1982) Low energy X-ray interaction coefficients: Photoabsorption, scattering and reflection. Atomic Data and Nuclear Data Tables **27**, 1-144.

[10] Leroux J, Thinh TP (1977) Revised Tables of X-ray Mass Absorption Coefficients. Claisse Scientific Corporation, Quebec, Canada.

[11] Liefield RJ (1968) Soft X-ray emission spectra at threshold excitation. In: Soft X-ray Band Spectra. Fabian DJ (ed.) Academic Press, 133-149.

[12] Pouchou JL, Pichoir F (1984) Un nouveau modèle de calcul pour la microanalyse quantitative par spectrométrie de rayons X. Partie I: application à l'analyse d'échantillons homogènes (A new correction model for electron probe microanalysis. Part I: Bulk specimens). La Recherche Aerospatiale **3**, 167-192.

[13] Pouchou JL, Pichoir F (1985) Anomalies d'émission et d'absorption du rayonnement Ni $L\alpha$ (Emission and absorption anomalies for Ni $L\alpha$ radiation). J. Microsc. Spectrosc. Electron. **10**, 291-294.

[14] Rémond G, Campbell JL, Packwood RH, Fialin M (1993) Spectral decomposition of wavelength dispersive x-ray spectra: Implications for quantitative analysis in the electron probe microanalyzer. Scanning Microscopy Supplement 7, (this volume).

[15] Urch DS (1970) The origin and intensities of low energy satellite lines in X-ray emission spectra: A

molecular orbital interpretation. J. Phys. C **3**, 1275-1291.

Discussion with Reviewers

J.L. Pouchou: In the example of the analysis of nitrogen in a Ti-N compound, it is implicitly assumed that the position and shape of the Ti Lι line are the same in the compound and in pure Ti. Is this assumption reasonable? Is it a source of significant error?

Authors: Indeed, Table 2 shows that significant differences exist for nitrogen measurements when either the peak or the peak integral modes are used.

Concerning the peak mode, Ti Lι counts are recorded from pure Ti at the peak position found for N Kα in the CrNx standard. No peak shift is noted, using the Ni/C multilayer monochromator, between the N Kα band in CrNx and the N Kα + Ti Li band in TiNOx. Nevertheless, the analytical mode leading to discrepancies, one may conclude that chemical effects modify the band shape of (1) N Kα in TiNOx compared to that in CrNx, and/or (2) Ti Li in TiNOx compared to that in pure Ti. The same remarks hold for UC$_2$ in Figure 2.

Only the peak integral mode accounts for such chemical effects, no matter what the impact of these effects is on the line of interest, and gives satisfactory results.

J.L. Pouchou: Again in the case of Ti-N analysis, you mention that the surface titanium oxide layer on the overlapping standard introduces some error. Could you give an order of magnitude of this error for a typical titanium oxide thickness?

J.D. Brown: Since you are using a PAP approach to the corrections, the effect of the surface oxide (thin film) could be calculated and removed. Is there any reason why this was not done?

J.L. Lábár: The authors attribute the 5% error in the analysis of TiNOx to the surface of the pure Ti standard. They present no measurement to support this assumption. Did they measure the thickness of this surface oxide and did they calculate its effect on the analysis?

Authors: According to Goldstein *et al.* [6], the native oxide skin present on the surface of pure Ti is equivalent to a 7.3 nm thick TiO$_2$ film. The treatment of this problem through bulk matrix correction programs would lead to 1 and 2 wt% oxygen no matter which primary beam energy is used. So far, we have made no measurements to evaluate the loss in Ti Kα counts due to the oxidized surface layer on pure Ti. An improvement in the computer program presented here will allow us to address the thin film problems in EPMA.

J.L. Lábár: What criteria decide the selection of linear or parabolic interpolation for the background in the presented method? Is the selection automatic? Did the authors examine the effect of the type of interpolation on the results?

Authors: It is assumed in the method presented that the background can be adjusted by a monotonously decreasing branch of a parabola. As a consequence, the program rejects, with an automatic selection of the linear interpolation, the solution leading to (1) the presence of the curve minimum within the spectral range scanned, and (2) a negative curvature of the parabola.

Strong improvements are given by the parabolic interpolation of the background, particularly for the analysis of minor elements whose analyzed lines are in the neighborhood of major lines (e.g., the tail of Fe L$_{\alpha,\beta}$ strongly overlaps F Kα when the W/Si multilayer monochromator is used for fluorine analysis).

J.L. Lábár: What facts (calculations, etc.) make the authors anticipate that "As a consequence, fluorine analysis in topaz using LiF as the standard should lead to underestimated experimental k-ratios with respect to the calculated ones?

Authors: The intensity emitted in an emission line from the valence band is directly related to the density of valence electrons in considered atomic sites, see Bonnelle, [Bonnelle C (1987) X-ray spectroscopy. In: Annual Report C. The Royal Society of Chemistry, London, 201-272] for more details on X-ray spectroscopy theory. As a consequence, one expects, in the relevant example, that the radiative transition probability associated with fluorine atoms in topaz will be lower than in LiF, the charge transfer from neighbouring cations to F atoms being less complete in topaz (rather covalent) than in LiF (ionic).

J.L. Pouchou: In the example of CuFeS$_2$, your interpretation is based on the fact that you find at all voltages, when pure Cu is used as a reference, a constant relative deviation between the experimental data and the PAP computation. To be valid, this conclusion requires that it has been checked before that, with the method you adopt for intensity measurements and with the m.a.c. used in the software, the PAP model predicts a satisfactory variation with voltage of the Cu Lα intensity emerging from pure Cu. Did you check this point? If yes, for which self m.a.c. of Cu Lα?

Authors: All PAP computations for copper data reduction used a self m.a.c. for Cu Lα derived from your [12] emerging intensity versus accelerating voltage measurements, 1828 cm^2/g to be compared with the computed value in the software, 1690 cm^2/g. The use of the latter value for CuFeS$_2$/Cu would lead to increasing rel-

ative error with increasing voltage, from 8% at 5 kV to 15% at 30 kV.

J.L. Lábár: What is the authors' suggestion for the analysis of Cu by the L lines?

Authors: Lα and Lβ lines are by far the most intense among the L-series lines, and moreover, the only ones non-trivial for EPMA in the soft energy range. Any change observed, except those due to self-absorption effects, on the Lα + Lβ spectra emitted from the unknown and standard should be accounted for to obtain accurate k-ratios.

The method described in the paper considers both Lα and Lβ lines as parts of the same emission band. Peak shift and peak shape alteration which affect this band between the unknown and the standard are treated in the same way as chemical effects in light element analysis, i.e., through the APF concept. The main problem is the correction for self-absorption of the APF considered. The self-absorption effects are quantified by a parameter, named R_{self} in the text, which reflects changes in the calculated Lβ/Lα ratios between both specimens.

In practice, the APF is measured at different voltages and plotted versus the corresponding R_{self}. The expected APF, to be multiplied to the peak k-ratios previously measured, correspond to $R_{self} = 1$.

The method is, of course, unable to account for changes in radiative transition probabilities for the atomic species considered from a specimen to another. Nevertheless, these problems could be minimized if the unknown and the standard belong to the same class: conductors, semiconductors, insulators.

J.D. Brown: In connection with the L-series lines where self-absorption becomes important, one could correct for self-absorption to obtain constant k-ratios. Is sufficient data available to make this a possibility?

Authors: To obtain constant corrected k-ratios, i.e., independent on the primary beam energy, it is of great importance for the available set of atomic data to be accurately defined. For L-series lines where self-absorption becomes important, the self m.a.c. of the analyzed line must be adjusted to get agreement between calculated and measured k-ratios. In that case, the suitable self m.a.c. is intermediate between those of both Lα and Lβ lines. Moreover, it strongly depends on the concentration of the analyzed element within the unknown and the standard.

Your suggestion, although it leads to unrealistic self m.a.c.'s, would be an interesting alternative, easy-to-operate for routine analysis, to the method presented. Indeed, only two measurements would have to be performed at two accelerating voltages, say 10 kV and 25 kV, to correct with a satisfying accuracy for self-absorption effects.